4-2023

Short Warm Distribution Tails Accelerate the Increase of Humid-Heat Extremes Under Global Warming

Paul Loikith
Portland State University, ploikith@pdx.edu

Yianna Sotirios Bekris
Portland State University, yiabek@gmail.com

J. D. Neelin
University of California, Los Angeles

Citation Details

Bekris, Y., Loikith, P. C., & Neelin, J. D. (2023). Short warm distribution tails accelerate the increase of humidheat extremes under global warming. Geophysical Research Letters, 50, e2022GL102164. https://doi. org/10.1029/2022GL102164

AGU ADVANCING EARTH AND SPACE SCIENCE

Geophysical Research Letters®

RESEARCH LETTER
10.1029/2022GL102164

Short Warm Distribution Tails Accelerate the Increase of Humid-Heat Extremes Under Global Warming

Yianna Bekris[1,2], Paul C. Loikith[1], and J. David Neelin[3]

[1]Department of Geography, Portland State University, Portland, OR, USA, [2]School of the Environment, Washington State University Vancouver, Vancouver, WA, USA, [3]Department of Atmospheric and Oceanic Sciences, University of California Los Angeles, Los Angeles, CA, USA

Key Points:

- Shorter-than-Gaussian wet-bulb temperature distribution warm tails lead to faster increases in extreme exceedances under warming compared to a Gaussian tail
- CMIP6 models competently simulate observed characteristics of wet-bulb temperature frequency distribution shape compared to reanalysis
- Wet-bulb temperature distribution shape is largely preserved under projected warming

Supporting Information:

Supporting Information may be found in the online version of this article.

Correspondence to:

P. C. Loikith,
ploikith@pdx.edu

Citation:

Bekris, Y., Loikith, P. C., & Neelin, J. D. (2023). Short warm distribution tails accelerate the increase of humid-heat extremes under global warming. *Geophysical Research Letters*, *50*, e2022GL102164. https://doi.org/10.1029/2022GL102164

Received 17 NOV 2022
Accepted 12 APR 2023

Author Contributions:

Conceptualization: Yianna Bekris, Paul C. Loikith, J. David Neelin
Data curation: Yianna Bekris
Formal analysis: Yianna Bekris
Funding acquisition: Paul C. Loikith, J. David Neelin
Investigation: Yianna Bekris
Methodology: Yianna Bekris, Paul C. Loikith, J. David Neelin
Resources: Paul C. Loikith
Software: Yianna Bekris
Supervision: Paul C. Loikith, J. David Neelin

Abstract Humid-heat extremes threaten human health and are increasing in frequency with global warming, so elucidating factors affecting their rate of change is critical. We investigate the role of wet-bulb temperature (T_W) frequency distribution tail shape on the rate of increase in extreme T_W threshold exceedances under 2°C global warming. Results indicate that non-Gaussian T_W distribution tails are common worldwide across extensive, spatially coherent regions. More rapid increases in the number of days exceeding the historical 95th percentile are projected in locations with shorter-than-Gaussian warm side tails. Asymmetry in the specific humidity distribution, one component of T_W, is more closely correlated with T_W tail shape than temperature, suggesting that humidity climatology strongly influences the rate of future changes in T_W extremes. Short non-Gaussian T_W warm tails have notable implications for dangerous humid-heat in regions where current-climate T_W extremes approach human safety limits.

Plain Language Summary Extreme heat is more dangerous to humans when it is combined with high humidity, so it is important to understand how the combination of heat and humidity will change under continued global warming. We investigate how the current distribution of wet-bulb temperatures, a heat-humidity measure, influences how future wet-bulb temperature extremes will increase. Results show that locations with an asymmetrical wet-bulb temperature probability distribution, such that the warm side of the distribution is shorter than if the distribution were normally shaped, are likely to see a faster increase in extreme wet-bulb temperature days under the same warming compared with other locations. Results suggest that the underlying humidity climatology is a more important driver of this distribution asymmetry compared to the underlying temperature climatology.

1. Introduction

Anthropogenic global warming is amplifying extreme heat (IPCC, 2021; Perkins et al., 2012), one of the deadliest types of severe weather (Barriopedro et al., 2011; Buzan et al., 2015; Robine et al., 2008). Future warming is confidently projected to further increase the frequency, severity, and extent of extreme heat events (Alexander et al., 2006; Mora et al., 2017), even under a relatively modest 1.5°C warming above mean preindustrial temperature (Dosio et al., 2018). In addition to high temperature, concurrent high humidity can enhance human heat stress (Buzan & Huber, 2020; Davis et al., 2016; Sherwood & Huber, 2010; Wheeler, 1991), as demonstrated by observed extreme humid-heat events with high death tolls (Barriopedro et al., 2011; Fischer & Knutti, 2013; Karl & Knight, 1997; Raymond et al., 2020; Wehner et al., 2016). Extreme humid-heat is similarly projected to increase in frequency, magnitude, and duration with global warming (Barnston et al., 2020; Coffel et al., 2017).

Wet-bulb temperature (T_W) is a heat-humidity quantity defined as the lowest temperature achievable through the saturation of water into an air parcel at constant pressure. Sherwood and Huber (2010) proposed that a T_W of 35°C, approximately human body temperature, is an unequivocal human adaptability threshold as evaporative cooling through sweating becomes insufficient to regulate body temperature. The identification of this upper adaptability limit has galvanized the study of extreme humid-heat (Buzan & Huber, 2020; Coumou & Robinson, 2013; Matthews, 2018; Pal & Eltahir, 2016; Raymond et al., 2020; Y. Zhang et al., 2021). When the 35°C T_W threshold was introduced in 2010, climate models showed that it would likely not be reached until approximately 7°C global warming (Sherwood & Huber, 2010). However, Raymond et al. (2020) discovered several instances exceeding 35°C T_W in weather station data, and Matthews (2018) identified a maximum of 35.4°C T_W at the hourly resolution in ERA5 reanalysis.

Validation: Yianna Bekris, Paul C. Loikith, J. David Neelin
Visualization: Yianna Bekris
Writing – original draft: Yianna Bekris
Writing – review & editing: Yianna Bekris, Paul C. Loikith, J. David Neelin

The 35°C T_W threshold is specific to a still, naked human, possibly underestimating heat stress in real-world conditions (Vanos et al., 2020). There is also scant experimental physiological research that substantiates this theoretical limit, but a recent experiment found young, healthy subjects' body temperatures began to rise at 31°C T_W and sometimes as low as 26°C T_W (Vecellio et al., 2022). Furthermore, coincident high humidity and heat has produced higher levels of morbidity and mortality in comparison to high heat alone, despite being substantially below the theoretical adaptability limit (Fischer & Knutti, 2013; Mora et al., 2017; Schär, 2016).

Considering that climate change is already increasing the occurrence of dangerous T_W extremes (Matthews, 2018; Raymond et al., 2020), improving our understanding of their changing frequency and severity is prudent. Anthropogenic temperature increases tend to be nonlinear and are not spatially uniform with respect to global mean temperature changes (Friedrich et al., 2016; Huybers et al., 2014; Loikith et al., 2018; Seneviratne et al., 2016), but T_W includes the added parameter of humidity, rendering the increase of T_W more complex. Humidity affects the partitioning of latent and sensible heat flux which impacts localized warming (Miralles et al., 2014; Seneviratne et al., 2010; Skinner et al., 2018), and paradoxically increases in T_W magnitude may differ from those of temperature during local extreme heat events (Coffel et al., 2019). Atmospheric dynamics may temper an increase of T_W extremes with global increases in temperature in the tropics (Sherwood & Huber, 2010; Y. Zhang et al., 2021), with climate models projecting regional increases of approximately 1°C in T_W per 1°C global increase in average dry-bulb temperature (Y. Zhang et al., 2021). Rastogi et al. (2020) found that for heatwaves with anomalously high values of the heat-humidity metric Apparent Temperature, there was an increase in temperature but relative humidity stayed the same, in contrast to relative humidity decreasing during dry heatwaves. There is also evidence that humidity sources, such as soil moisture, can influence the shape of the temperature probability density function (Berg et al., 2014; Zscheischler & Seneviratne, 2017). These inherent complexities confound the projection of future increases in extreme T_W.

Another complicating factor in the increase of T_W extremes is the shape of the T_W probability distribution. The non-Gaussian nature of temperature climatology is well-established (Catalano et al., 2021; Garfinkel & Harnik, 2017; Linz et al., 2018; Perron & Sura, 2013; Simolo et al., 2010, 2011; B. Zhang et al., 2022), and some physical explanations have been offered, generally related to underlying horizontal temperature gradients (Catalano et al., 2021; Garfinkel & Harnik, 2017; Linz et al., 2018; Perron & Sura, 2013), but non-Gaussianity in T_W distributions has not been explored to our knowledge. Tail shape relative to a Gaussian strongly influences the rate of changes in exceedances over a fixed extreme temperature threshold, and a shorter-than-Gaussian warm tail can lead to a greater increase in extreme warm exceedances under global warming than if the tail were Gaussian or longer (Loikith et al., 2018; Loikith and Neelin, 2015, 2019; Ruff & Neelin, 2012). We investigate the global prevalence of T_W, temperature, and specific humidity (q) non-Gaussian tails and their influence on future T_W exceedances above the current-climate 95th percentile extreme threshold under 2°C global warming.

2. Data

We utilized 31 models contributing to the sixth phase of the Coupled Model Intercomparison Project (CMIP6; Eyring et al., 2016; Table S1 in Supporting Information S1) which were validated against reanalysis from the Modern-Era Retrospective analysis for Research and Applications, Version 2 (MERRA-2; Gelaro et al., 2017). Models were selected based on the availability of the necessary meteorological variables (specific humidity, dry-bulb temperature, and pressure) for T_W calculation, and MERRA-2 variables used for calculating T_W were specific humidity, 2m temperature, and surface pressure. Scenarios from CMIP6 included the preindustrial control (piControl), historical, and the highest emission scenario, ssp585. The first ensemble member of each model was used when more than one was available. Both CMIP6 models and MERRA-2 data were regridded from their native resolutions (CMIP6 model resolutions in Table S2 in Supporting Information S1; MERRA-2 native resolution is 0.5° latitude by 0.625° longitude) to a 2° latitude by 2° longitude resolution using bilinear interpolation, and resampled from hourly values to a daily mean. Some results were also compared against the ERA5 reanalysis which is provided on a 0.25° latitude-longitude grid (Hersbach et al., 2020). All land masses with the exception of Antarctica are included.

3. Methodology

T_W was calculated using a Python translation (Li, 2019) of a Matlab implementation (Kopp, 2016) of the Davies-Jones (2008) method utilizing pseudoadiabats and employed by Buzan et al. (2015). This method is

accurate up to 40°C T_W (Davies-Jones, 2008). We compared historical multi-model ensemble mean (MMEM) results with MERRA-2 data for 1985–2014. T_W anomaly distributions for June–July–August (JJA) and December–January–February (DJF) were created for each model for the historical period of 1985–2014 and the MERRA-2 dataset at each grid cell. Anomalies were constructed by subtracting the daily T_W climatology computed over the entire historical period from each day separately for each dataset. Gaussianity was assessed through a *shift ratio*, which is obtained by shifting each distribution by 0.5 standard deviations (σ), counting the increase in days exceeding the pre-shifted 95th percentile, and dividing by the increase expected from an equivalently shifted Gaussian distribution as detailed by Catalano et al. (2020). If the shift ratio is greater than one, the tail is shorter-than-Gaussian, and longer if the shift ratio is less than one.

The expected increase in threshold exceedances from a Gaussian is computed by shifting a Gaussian distribution 0.5σ 10,000 times and finding the median of these shifts. A warm tail is deemed statistically significantly different from Gaussian if the increase in exceedances after the shift falls above the 95th percentile of the 10,000 shift values. The distribution is shifted by 0.5σ instead of a fixed value to ensure the shift is proportional to the width of the distribution This approach serves as a variant of the Kolmogorov–Smirnov/Lilliefors test for normality (Loikith & Neelin, 2015) and differs from measuring skewness as it is applicable to more symmetrical distributions which have short or long tails on both sides of the distribution.

We computed a pre-industrial baseline global average temperature (1850–1900) to identify the initial 30-year period in which each model simulates 2°C time-average warming of global mean surface air temperature (Table S1 in Supporting Information S1), which acts as our future period. This helps compensate for differences in equilibrium climate sensitivity, which is highly variable within CMIP6 (Zelinka et al., 2020), thus constraining the range of warming magnitudes relative to the historical period. Any future warming scenario in which all models reach a global warming of 2°C above the preindustrial mean could be used, however we used the ssp585 scenario here. To assess the influence of historical tail shape on future extreme exceedances, we calculate a *warming ratio* (as in Loikith et al., 2018) at each grid cell for each climate model using the following procedure:

1. Calculate the exceedances of the 1985–2014 95th percentile of T_W for the future period.
2. Shift a Gaussian distribution by the simulated mean warming (in σ) between the historical and future periods, and calculate the exceedances of the pre-shifted 95th percentile.
3. Divide the value from step #1 by step #2 to obtain the *warming ratio*.

A warming ratio greater than one denotes a larger increase in extreme T_W exceedances than expected from warming a Gaussian by the same amount. We note that models which warm faster are closer to the 2°C threshold above the preindustrial baseline by the 1985–2014 reference period than models that warm slower. In all cases, warming magnitude is relatively modest and realistic within the near future, allowing for a pragmatic illustration of the effects of non-Gaussian warm side T_W tails under near-future warming.

4. Results

4.1. Global Analysis

As with temperature (Linz et al., 2018; Loikith et al., 2018; Loikith & Neelin, 2019; Ruff & Neelin, 2012), results indicate extensive, spatially coherent regions of non-Gaussian T_W warm side tails worldwide in both CMIP6 and MERRA-2 (Figure 1). Regions with short tails extend across both the northern and southern hemispheres in JJA and DJF. For relevance to impacts, we focus primarily on short tail regions in the summer season in the extratropics, along with the tropics in both seasons. Some notable summer examples of short tailed regions in MERRA-2 (Figures 1a and 1b) are the southeastern United States, southern Europe and parts of Southeast Asia in JJA, and central South America, southern Africa and northern Australia in DJF. Prior research on dry-bulb temperature distributions suggests that short tails are expected to be most impactful on future increases in threshold exceedances in regions with hotter T_W climatologies (Loikith et al., 2018; Loikith & Neelin, 2015; Ruff & Neelin, 2012), such as the southeastern United States. Long tails are also prevalent across the Sahara in DJF and the Arabian Peninsula in JJA, although these are not as widespread as short tails. A possible explanation for these long tails is the close spatiotemporal relationship between precipitation and extreme humid-heat days in this region (Speizer et al., 2022).

Comparison of MERRA-2 shift ratios with those of the CMIP6 MMEM (Figures 1c and 1d) reveals that the MMEM realistically captures the reanalysis shift ratio patterns. For example, the short tails in the southeastern

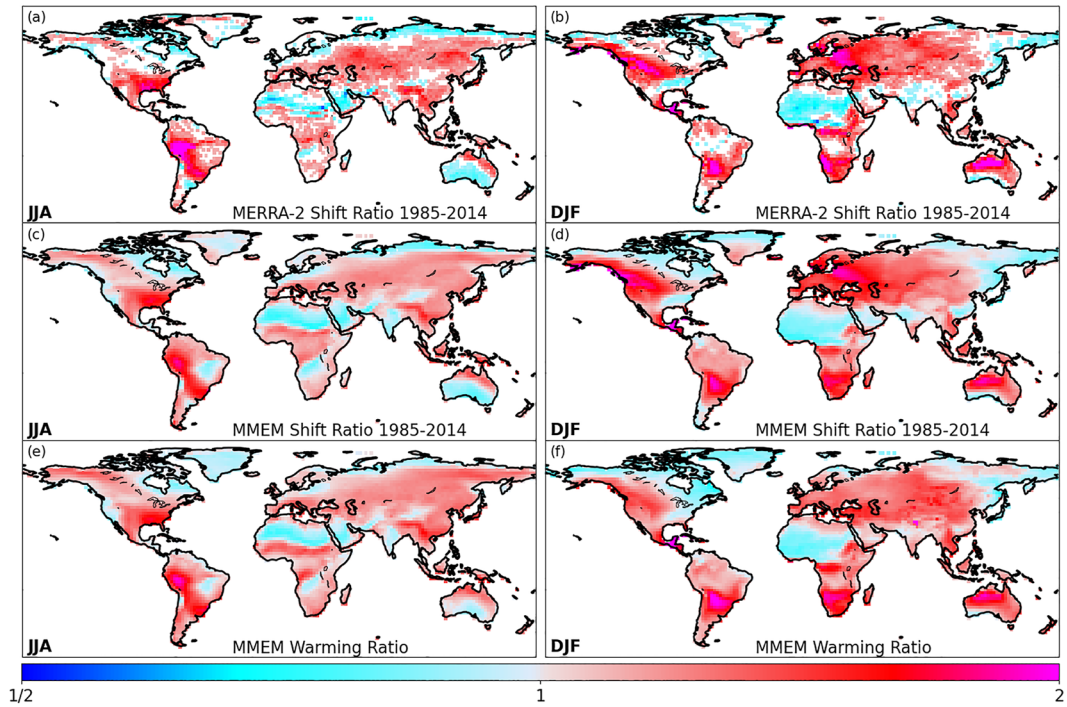

Figure 1. Wet-bulb temperature shift ratio maps for (a–b) MERRA-2 reanalysis and (c–d) the CMIP6 multi-model ensemble mean (MMEM) based on distributions for 1985–2014. Values larger than one (red hues) indicate a short tail at high temperatures and a larger number of exceedances than if the shifted distribution were Gaussian. Values less than one (blue hues) signify a long tail and a lower number of exceedances than if the shifted distribution were Gaussian. White grid cells on land in MERRA-2 represent a warm-tail that is not significantly different from a Gaussian. (e–f) Warming ratio maps for the CMIP6 MMEM comparing CMIP6 projections at 2°C warming (see text) to a Gaussian shifted by the same mean warming relative to the 1985–2014 historical period. Color conventions as for (a–d).

United States, across Europe, and throughout central America in JJA closely resemble reanalysis as do the short tails in northern Australia and Central America in DJF. There are some locations with less agreement, such as the long tails in the MMEM over India in JJA. Because the MMEM includes 31 models, some variability and magnitude may be reduced compared to individual models. In a few regions, a broad area that is mostly Gaussian according to MERRA-2 can appear non-Gaussian in the MMEM, such as across the Amazon basin and the northern Sahara desert. Despite these caveats, the patterns of short and long tails are spatially similar between the reanalysis and climate model data, including when comparing individual models (not shown).

Figure 1 (bottom row) shows maps of the CMIP6 MMEM warming ratio, with values greater than one indicating a larger projected increase in extreme T_W threshold exceedances than expected from shifting a Gaussian by the same mean warming. The close correspondence between the shift and warming ratios in Figure 1 highlights the important role tail shape plays in the rate of increase in extreme threshold exceedances. In general, regions with shorter-than-Gaussian warm tails are projected to see faster-than-Gaussian increases in extreme warm T_W threshold exceedances while regions with longer-than-Gaussian warm tails are projected to see a slower increase. While the warming ratios have more variation between models comprising the MMEM than the shift ratios (not shown), spatial patterns were mostly similar. There are some exceptions to the accordance between tail Gaussianity and warming ratios, such as the central-western and southeastern coast of Australia in JJA and the southeastern United States in DJF. Elsewhere, there is only subtle incongruence between the shift ratio and warming ratio, exemplified by their coincident extent across the entirety of North America in JJA, South America in DJF, Australia in DJF, Africa in DJF, and Southeast Asia in JJA.

While short tails are projected to lead to a faster increase in the frequency of days that exceed the historical extreme warm threshold, for areas with long tails, extreme threshold exceedances can be far above the mean, and possibly dangerously high in some locations such as parts of the Arabian Peninsula or parts of India in JJA (Im et al., 2017; van Oldenborgh et al., 2018). These locations may be the most at-risk of exceeding the 35°C

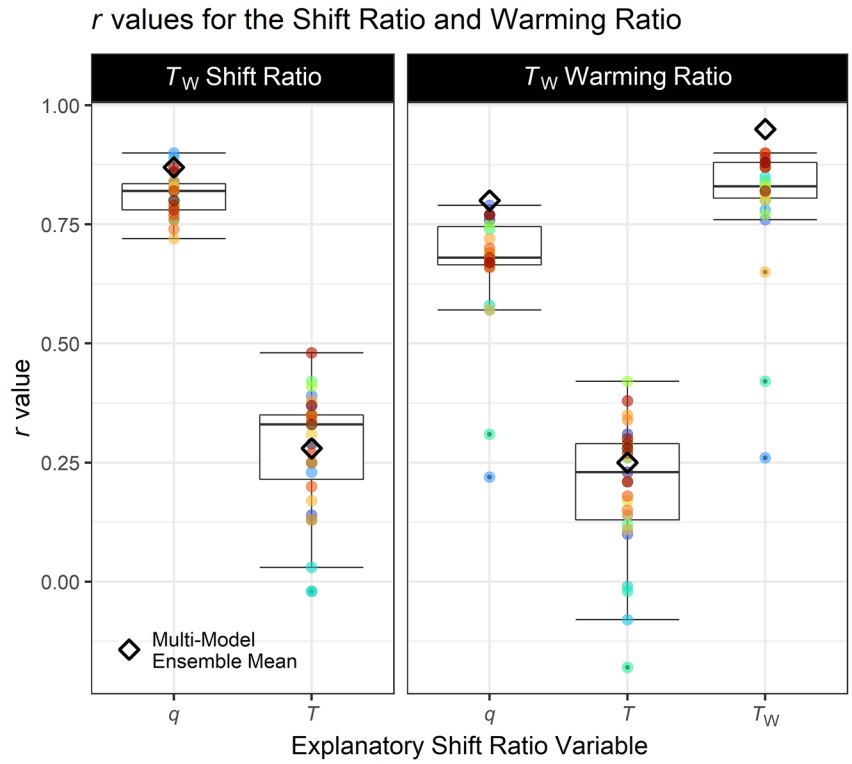

Figure 2. A visual summary of the linear regression coefficients for the T_W shift ratio, air temperature (T) shift ratio, and specific humidity (q) shift ratio, and the T_W warming ratio, matched to each grid cell in each dataset. Each point represents an individual CMIP6 model, and the black diamond represents the multi-model ensemble mean. All p-values are under 0.05. Only grid cells on land for June–July–August in the northern hemisphere and December–January–February in the southern hemisphere were included. A table of the values used to construct this figure are in Supporting Information S1 (Table S2 in Supporting Information S1).

adaptability threshold under warming, even though the increase in exceedances frequency will be slower than if the tail was Gaussian or shorter. Other long tailed locations may be exposed to extreme high T_W that are so anomalous that existing infrastructure is lacking in its ability to safely cool the population. In this sense, long tails may assist in the identification of areas which are at risk of very rare, but very large, excursions from the mean.

To quantify the influence of the shift ratio on the projected change in exceedance frequency, we performed a series of linear regressions between the shift ratio and warming ratio maps for each model, as well as the MMEM, and similarly for shift ratio maps of the two primary components of T_W, temperature and q (Figure 2). The correlation between the shift ratio and projected exceedances is at its strongest when utilizing the T_W shift ratio ($r = 0.95$; Table S2 in Supporting Information S1), but the relative roles of temperature and q are also meaningful. While the non-Gaussianity of T_W sometimes follows the pattern of temperature non-Gaussianity (Figures S1 and S2 in Supporting Information S1), our analysis suggests that q has a more direct influence on T_W distribution shape than temperature. This closer relationship between q and T_W is in accordance with prior work (Buzan & Huber, 2020; Matthews et al., 2022; Raymond et al., 2017). The temperature shift ratio is only weakly correlated with the T_W warming ratio ($r = 0.25$; Table S2 in Supporting Information S1), while the shift ratio for q is more closely correlated ($r = 0.80$; Table S2 in Supporting Information S1). There is some variability between models worth noting. CNRM-CM6-1, CNRM-CM6-1-HR, CNRM-ESM2-1, and EC-Earth3 show a weak negative correlation between the temperature shift ratio and the warming ratio, while CNRM-CM6-1 and CNRM-ESM2-1 also have a weak negative correlation between temperature shift ratio and the T_W shift ratio (Table S2 in Supporting Information S1). All other models in our analysis exhibit similar patterns of correlation. It is reasonable to assume some uncertainty in the ability of the models to simulate future changes in both temperature and humidity, especially in places where changes in q may result from complex interactions between the land and atmosphere (McKinnon & Poppick, 2020). However, the fact that non-Gaussianity in the underlying q distribution is a strong indicator of future change in T_W extremes is consistent with Clausius-Clapeyron scaling (Held & Soden, 2000; Santer

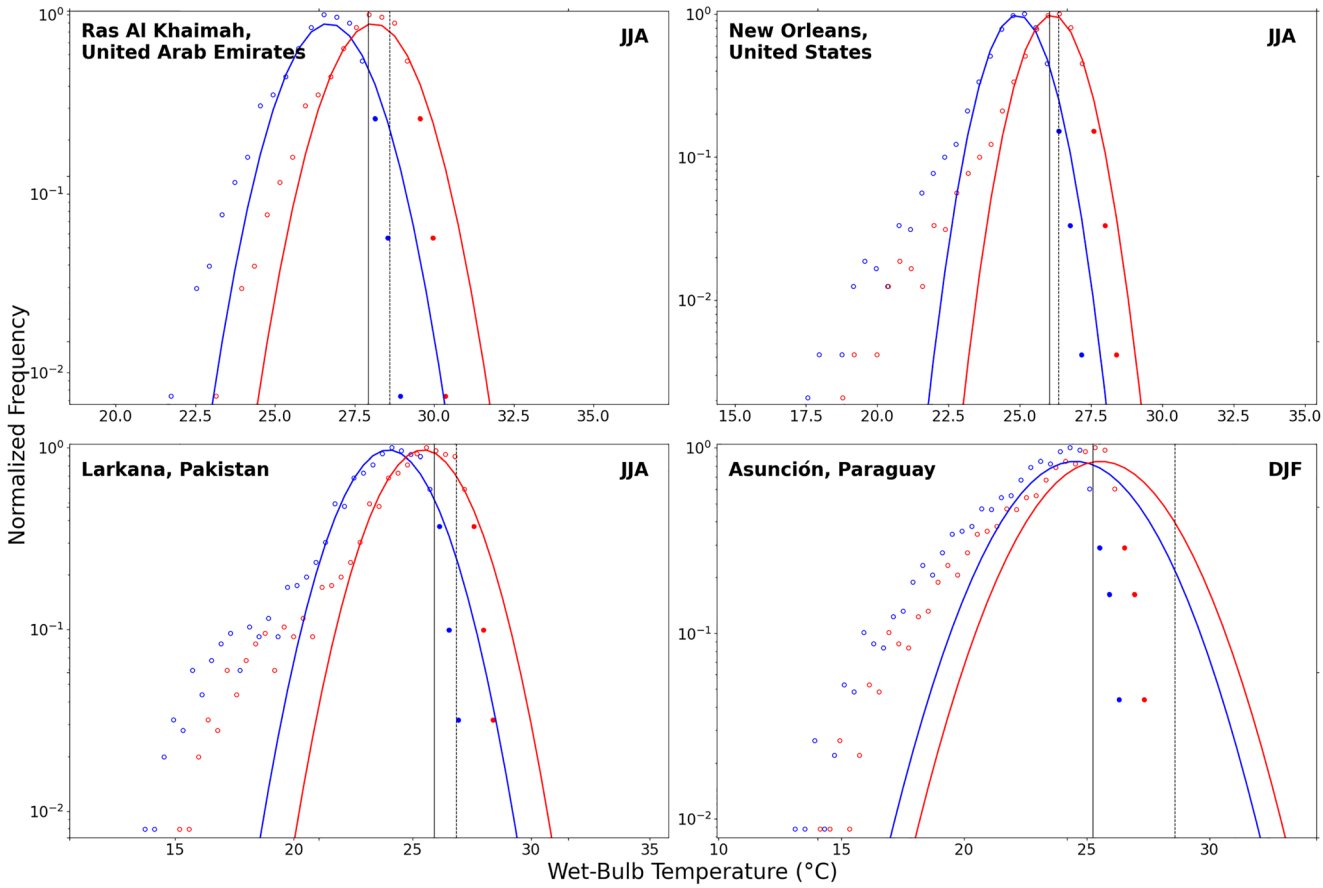

Figure 3. Rigidly shifted MERRA-2 probability distributions of 1985–2014 T_W with a Gaussian curve fit to the core, plotted on a log scale. In each subplot, the vertical solid line indicates the historical 95th percentile, the vertical dashed line is the historical Gaussian 95th percentile, and points are histogram bin centers. Solid points represent the warm-tail. Panel (a) is Ras Al Khaimah in the United Arab Emirates on the Persian Gulf coast in June–July–August (JJA), panel (b) is New Orleans, Louisiana in the United States in JJA, panel (c) is Larkana, Pakistan in JJA, and panel (d) is Asunción, Paraguay, in December–January–February.

et al., 2007; Willet et al., 2007), although q may not always be expected to scale with temperature increases (Coffel et al., 2019). We find that the shift ratio spatial patterns for q and T are similar between the MMEM and MERRA-2 (Figures S1 and S2 in Supporting Information S1).

4.2. Regional Analysis

Historical and future T_W distributions for four short tailed locations are shown in Figure 3 with Gaussian fits to the core provided to visualize the departures from Gaussian in the tails (following Loikith & Neelin, 2015). The historical (blue) distribution is from MERRA-2 for the grid cell closest to the indicated city. For comparison with a higher resolution reanalysis, the same plots are provided using ERA5 reanalysis in Figure S6 in Supporting Information S1 which qualitatively agree well with MERRA-2. This distribution is shifted by the MMEM projected warming (in σ) for that grid cell, computed between the historical and future periods (as in Figures S7 and S8 in Supporting Information S1). This is a uniform shift which assumes no changes in variance, skewness, or kurtosis. This is consistent with the very little change seen in the shift ratios under 2°C warming as simulated by the models (Figure S3 in Supporting Information S1).

We chose four locations to represent a range of climatological conditions, each with shorter-than-Gaussian warm tails, and each with a 95th percentile T_W warmer than 25°C in the current climate. Ras Al Khaimah, United Arab Emirates is within a narrow coastally confined region of short tails along the Persian Gulf and has the hottest 95th percentile. It represents a region where global warming may lead to dangerous T_W extremes (Raymond et al., 2020). New Orleans, United States, has a humid, hot summer climate, influenced by its proximity to the Gulf of Mexico and is located within a broad region of short tails. Larkana, Pakistan is located along the Indus

River, north of the Arabian Sea within a spatially small short tailed region, and Asunción, Paraguay is an inland location in subtropical South America within a region of notably short warm tails. While geographically diverse, all four locations are within the subtropics with nearby or regional sources of moisture resulting in very warm T_W. The presence of short warm tails is likely related to the proximity to large bodies of water for Ras Al Khaimah, New Orleans, and Larkana, as the water bodies exert an upper limit on humidity and temperature. The short tail at Asunción may be related to warm and humid environments being conducive to convection in the region, limiting T_W excursions from the mean on the warm side, however this is only speculative.

Ras Al Khaimah displays a shift in extreme T_W days translating to a substantial portion of the summer months being of high risk to human heat stress, with a projected 58.4% of days over the historical 95th percentile threshold of 27.3°C T_W (Figure 3a). New Orleans, Larkana, and Asunción, also are projected to see a large rise in summer extreme humid-heat days (Figures 3b–3d). Their percentage of days over their current-climate 95th percentiles (New Orleans: 26°C T_W; Larkana: 25.9°C T_W; Asunción: 25.3°C T_W) is projected to be 51.1%, 29%, and 20.3%, respectively under this range of CMIP6 warming magnitudes benchmarked at the point when each model simulates 2°C of global warming relative to the preindustrial baseline. These four locations can be viewed as representative of their respective regions where a combination of short warm side tails and an underlying very warm T_W climatology lead to a rapid increase in dangerous T_W under relatively modest global warming.

In some locations, especially for those with relatively low T_W variance (Figures S4 and S5 in Supporting Information S1), the recent-climate 95th percentile will be exceeded most of the time under this relatively modest amount of mean warming. In these locations, tail shape is not as relevant to the rate of increase because a small amount of warming will shift most of the distribution to the right of the 95th percentile. Therefore, we have only included examples of locations with sufficiently large variance (σ greater than 1°C) for tail shape to influence future increases in extreme threshold exceedances. To illustrate this effect for cases where warming will lead to a very large number of days exceeding the historical extreme threshold, but where variance is small and the influence of warm-tail shape is dampened, we provide some examples in Supporting Information S1 (Figure S7 in Supporting Information S1).

5. Discussion and Conclusions

Since the identification of a theoretical physiological upper limit of T_W (Sherwood & Huber, 2010), much attention has been paid to the intensification of humid-heat extremes under global warming (Matthews, 2018; Pal & Eltahir, 2016; Raymond et al., 2020; Schär, 2016). Climate model studies analyzing future T_W extremes often focus on global warming far above 2°C, such as 4°C (Schär, 2016), or even 7°C (Sherwood & Huber, 2010) relative to the preindustrial baseline, or during the 30-year period of 2071–2100 when some CMIP6 models simulate a similarly high amount of warming under high-end emissions scenarios (Coffel et al., 2017; Pal & Eltahir, 2016). There are also several studies which examine T_W at different emissions levels (Chen et al., 2022) and others under 1.5°C, 2°C warming, and 3°C (Freychet et al., 2022; Saeed et al., 2021; X.-S. Wang et al., 2022). While these studies have an emphasis on the adaptability threshold of 35°C, we emphasize areas that may be regularly exposed to T_W values which are considered extreme in the recent climatology. An overemphasis on the 35°C T_W threshold may overlook locations which are at high risk of dangerous humid-heat stress in the near future, even if T_W values may not approach the adaptability limit.

Some analyses of increases in humid-heat extremes assume Gaussianity of the underlying distributions at each location, identifying significant shifts up to 3σ in the time period of 2000–2012 in the tropics (Coumou & Robinson, 2013). We find that this similarly applies to non-Gaussian T_W distributions when σ is less than about 1°C, since even a modest warming shifts the core of the distribution to the right of the pre-shifted 95th percentile. We therefore focus our analysis on the subtropics and extratropics where T_W distribution tail shape is well-correlated with future extreme threshold exceedances. It is further theorized that within the tropics, T_W warming may be limited to 1°C per 1°C tropical mean warming, possibly preventing extremes from reaching the 35°C threshold (Y. Zhang et al., 2021), although this hypothesis is disputed in regional analyses (Raymond et al., 2020, 2021). Even if 35°C may not be reached, a daily mean T_W almost always above 26°C would create substantial public health and infrastructure challenges as illustrated for Cancún, Mexico and Darwin, Australia (Figure S6 in Supporting Information S1). In addition, our analysis utilizes a daily mean instead of a maximum T_W, so a breach of the adaptability threshold cannot be ruled out. A very high daily mean T_W can also be suggestive of high nighttime T_W, prolonging exposure to heat stress (Kravchenko et al., 2013). It is possible that in some

cases, the prevailing meteorology that causes the short tails may also prevent T_W from becoming too high, such as is seen with temperature distributions (Catalano et al., 2021).

The relative contributions of humidity and heat to the risk of human heat stress is still under active study (Lutsko, 2021). Prior research suggests that latitude, topography (Raymond et al., 2022), or other geographic and climatological factors (Buzan et al., 2015; Ivanovich et al., 2022; Raymond et al., 2017; P. Wang et al., 2019; Zhao et al., 2015) can all be influential. Buzan and Huber (2020) found that T_W generally aligned with extreme humidity, but Heat Index and simple wet-bulb globe temperature aligned with temperature. In agreement with Fischer and Knutti (2013), our analysis supports that heat and humidity combined provide a more robust assessment of T_W. We also find that specific humidity has a larger contribution to projected T_W extremes than temperature when assessed using our shift ratio methodology. The physical mechanisms behind this are outside the scope of this study, but a more thorough understanding of how specific humidity and temperature interact to produce T_W extremes may benefit the accurate projection of their future occurrence.

This study effectively demonstrates that departures from Gaussianity on the warm side of the T_W probability distribution influence the projected rate of change in extreme threshold exceedances under future warming. Short warm tails are of particular concern as they may indicate a very large number of future exceedances over the current-climate 95th percentile. Although this analysis suggests that long tails result in a slower increase in exceedances in comparison to Gaussian or shorter tails, long tails can still be impactful in areas unprepared for extreme T_W due to its relative rarity. While certain short tailed locations might endure persistently dangerous T_W during the warm season, it is possible that long tailed locations might experience T_W that the local populace may be unprepared for (Guirguis et al., 2018). Insight into the changing probability of extreme T_W and identifying locations at risk of dangerous T_Ws is essential in the adequate preparation for the human health and societal consequences of extreme humid-heat under global warming.

Data Availability Statement

MERRA-2 data were obtained from the Goddard Earth Sciences (GES) Data and Information Services Center (DISC) website (http://disc.sci.gsfc.nasa.gov/mdisc/) and CMIP6 were downloaded from the World Climate Research Program (WCRP) website hosted by Earth System Grid Federation (ESGF) (https://esgf-node.llnl.gov/projects/cmip6/). CMIP6 models analyzed are in Table S1 in Supporting Information S1. ERA5 data are provided at https://climate.copernicus.eu/climate-reanalysis. Code used to conduct the presented analysis can be found at: https://github.com/yiabek/nongaussian_wetbulb_tails.

Acknowledgments
Support for this work is provided by the U.S. National Science Foundation through Grant AGS-1621554. We would like to thank Arielle Catalano for her contributions through software development. We thank Andrew Martin and Daniel Taylor Rodriguez for their helpful guidance. We also thank the reviewers for their very constructive comments.

References

Alexander, L. V., Zhang, X., Peterson, T. C., Caesar, J., Gleason, B., Tank, A. M. G. K., et al. (2006). Global observed changes in daily climate extremes of temperature and precipitation. *Journal of Geophysical Research*, *111*(D5), D05109. https://doi.org/10.1029/2005JD006290

Barnston, A. G., Lyon, B., Coffel, E. D., & Horton, R. M. (2020). Daily autocorrelation and mean temperature/moisture rise as determining factors for future heat-wave patterns in the United States. *Journal of Applied Meteorology and Climatology*, *59*(10), 1735–1754. https://doi.org/10.1175/JAMC-D-19-0291.1

Barriopedro, D., Fischer, E. M., Luterbacher, J., Trigo, R. M., & García-Herrera, R. (2011). The hot summer of 2010: Redrawing the temperature record map of Europe. *Science*, *332*(6026), 220–224. https://doi.org/10.1126/science.1201224

Berg, A., Lintner, B. R., Findell, K. L., Malyshev, S., Loikith, P. C., & Gentine, P. (2014). Impact of soil moisture–atmosphere interactions on surface temperature distribution. *Journal of Climate*, *27*(21), 7976–7993. https://doi.org/10.1175/JCLI-D-13-00591.1

Buzan, J. R., & Huber, M. (2020). Moist heat stress on a hotter Earth. *Annual Review of Earth and Planetary Sciences*, *48*(1), 623–655. https://doi.org/10.1146/annurev-earth-053018-060100

Buzan, J. R., Oleson, K., & Huber, M. (2015). Implementation and comparison of a suite of heat stress metrics within the Community Land Model version 4.5. *Geoscientific Model Development*, *8*(2), 151–170. https://doi.org/10.5194/gmd-8-151-2015

Catalano, A. J., Loikith, P. C., & Neelin, J. D. (2020). Evaluating CMIP6 model fidelity at simulating non-Gaussian temperature distribution tails. *Environmental Research Letters*, *15*(7), 074026. https://doi.org/10.1088/1748-9326/ab8cd0

Catalano, A. J., Loikith, P. C., & Neelin, J. D. (2021). Diagnosing non-Gaussian temperature distribution tails using back-trajectory analysis. *Journal of Geophysical Research: Atmospheres*, *126*(8), e2020JD033726. https://doi.org/10.1029/2020JD033726

Chen, H., He, W., Sun, J., & Chen, L. (2022). Increases of extreme heat-humidity days endanger future populations living in China. *Environmental Research Letters*, *17*(6), 064013. https://doi.org/10.1088/1748-9326/ac69fc

Coffel, E. D., Horton, R. M., & de Sherbinin, A. (2017). Temperature and humidity based projections of a rapid rise in global heat stress exposure during the 21st century. *Environmental Research Letters*, *13*(1), 014001. https://doi.org/10.1088/1748-9326/aaa00e

Coffel, E. D., Horton, R. M., Winter, J. M., & Mankin, J. S. (2019). Nonlinear increases in extreme temperatures paradoxically dampen increases in extreme humid-heat. *Environmental Research Letters*, *14*(8), 084003. https://doi.org/10.1088/1748-9326/ab28b7

Coumou, D., & Robinson, A. (2013). Historic and future increase in the global land area affected by monthly heat extremes. *Environmental Research Letters*, *8*(3), 034018. https://doi.org/10.1088/1748-9326/8/3/034018

Davies-Jones, R. (2008). An efficient and accurate method for computing the wet-bulb temperature along pseudoadiabats. *Monthly Weather Review*, *136*(7), 2764–2785. https://doi.org/10.1175/2007MWR2224.1

Davis, R. E., McGregor, G. R., & Enfield, K. B. (2016). Humidity: A review and primer on atmospheric moisture and human health. *Environmental Research*, *144*, 106–116. https://doi.org/10.1016/j.envres.2015.10.014

Dosio, A., Mentaschi, L., Fischer, E. M., & Wyser, K. (2018). Extreme heat waves under 1.5°C and 2°C global warming. *Environmental Research Letters*, *13*(5), 054006. https://doi.org/10.1088/1748-9326/aab827

Eyring, V., Bony, S., Meehl, G. A., Senior, C. A., Stevens, B., Stouffer, R. J., & Taylor, K. E. (2016). Overview of the coupled model intercomparison project phase 6 (CMIP6) experimental design and organization. *Geoscientific Model Development*, *9*(5), 1937–1958. https://doi.org/10.5194/gmd-9-1937-2016

Fischer, E. M., & Knutti, R. (2013). Robust projections of combined humidity and temperature extremes. *Nature Climate Change*, *3*(2), 126–130. https://doi.org/10.1038/nclimate1682

Freychet, N., Hegerl, G. C., Lord, N. S., Lo, Y. T. E., Mitchell, D., & Collins, M. (2022). Robust increase in population exposure to heat stress with increasing global warming. *Environmental Research Letters*, *17*(6), 064049. https://doi.org/10.1088/1748-9326/ac71b9

Friedrich, T., Timmermann, A., Tigchelaar, M., Elison Timm, O., & Ganopolski, A. (2016). Nonlinear climate sensitivity and its implications for future greenhouse warming. *Science Advances*, *2*(11), e1501923. https://doi.org/10.1126/sciadv.1501923

Garfinkel, C. I., & Harnik, N. (2017). The non-Gaussianity and spatial asymmetry of temperature extremes relative to the storm track: The role of horizontal advection. *Journal of Climate*, *30*(2), 445–464. https://doi.org/10.1175/JCLI-D-15-0806.1

Gelaro, R., McCarty, W., Suárez, M. J., Todling, R., Molod, A., Takacs, L., et al. (2017). The modern-era retrospective analysis for research and applications, version 2 (MERRA-2). *Journal of Climate*, *30*(14), 5419–5454. https://doi.org/10.1175/JCLI-D-16-0758.1

Guirguis, K., Gershunov, A., Cayan, D. R., & Pierce, D. W. (2018). Heat wave probability in the changing climate of the Southwest US. *Climate Dynamics*, *50*(9), 3853–3864. https://doi.org/10.1007/s00382-017-3850-3

Held, I. M., & Soden, B. J. (2000). Water vapor feedback and global warming. *Annual Review of Energy and the Environment*, *25*(1), 441–475. https://doi.org/10.1146/annurev.energy.25.1.441

Hersbach, H., Bell, B., Berrisford, P., Hirahara, S., Horányi, A., Muñoz-Sabater, J., et al. (2020). The ERA5 global reanalysis. *Quarterly Journal of the Royal Meteorological Society*, *146*(730), 1999–2049. https://doi.org/10.1002/qj.3803

Huybers, P., McKinnon, K. A., Rhines, A., & Tingley, M. (2014). U.S. daily temperatures: The meaning of extremes in the context of nonnormality. *Journal of Climate*, *27*(19), 7368–7384. https://doi.org/10.1175/JCLI-D-14-00216.1

Im, E.-S., Pal, J. S., & Eltahir, E. A. B. (2017). Deadly heat waves projected in the densely populated agricultural regions of South Asia. *Science Advances*, *3*(8), e1603322. https://doi.org/10.1126/sciadv.1603322

IPCC. (2021). In V. Masson-Delmotte, P. Zhai, A. Pirani, S. L. Connors, C. Péan, et al. (Eds.), *Climate change 2021: The physical science basis. Contribution of Working Group I to the sixth assessment report of the Intergovernmental Panel on Climate Change*. Cambridge University Press. (In Press). https://doi.org/10.1017/9781009157896

Ivanovich, C., Anderson, W., Horton, R., Raymond, C., & Sobel, A. (2022). The influence of intraseasonal oscillations on humid-heat in the Persian Gulf and South Asia. *Journal of Climate*, *35*(13), 4309–4329. https://doi.org/10.1175/JCLI-D-21-0488.1

Karl, T. R., & Knight, R. W. (1997). The 1995 Chicago heat wave: How likely is a recurrence? *Bulletin of the American Meteorological Society*, *78*(6), 1107–1120. https://doi.org/10.1175/1520-0477(1997)078<1107:TCHWHL>2.0.CO;2

Kopp, B. (2016). WetBulb.m. Retrieved from https://github.com/bobkopp/WetBulb.m

Kravchenko, J., Abernethy, A. P., Fawzy, M., & Lyerly, H. K. (2013). Minimization of heatwave morbidity and mortality. *American Journal of Preventive Medicine*, *44*(3), 274–282. https://doi.org/10.1016/j.amepre.2012.11.015

Li, X. (2019). WetBulb.py. Retrieved from https://github.com/smartlixx/WetBulb

Linz, M., Chen, G., & Hu, Z. (2018). Large-scale atmospheric control on non-Gaussian tails of midlatitude temperature distributions. *Geophysical Research Letters*, *45*(17), 9141–9149. https://doi.org/10.1029/2018GL079324

Loikith, P. C., & Neelin, J. D. (2015). Short-tailed temperature distributions over North America and implications for future changes in extremes. *Geophysical Research Letters*, *42*(20), 8577–8585. https://doi.org/10.1002/2015GL065602

Loikith, P. C., & Neelin, J. D. (2019). Non-Gaussian cold-side temperature distribution tails and associated synoptic meteorology. *Journal of Climate*, *32*(23), 8399–8414. https://doi.org/10.1175/JCLI-D-19-0344.1

Loikith, P. C., Neelin, J. D., Meyerson, J., & Hunter, J. S. (2018). Short warm-side temperature distribution tails drive hot spots of warm temperature extreme increases under near-future warming. *Journal of Climate*, *31*(23), 9469–9487. https://doi.org/10.1175/JCLI-D-17-0878.1

Lutsko, N. J. (2021). The relative contributions of temperature and moisture to heat stress changes under warming. *Journal of Climate*, *34*(3), 901–917. https://doi.org/10.1175/JCLI-D-20-0262.1

Matthews, T. (2018). Humid-heat and climate change. *Progress in Physical Geography: Earth and Environment*, *42*(3), 391–405. https://doi.org/10.1177/0309133318776490

Matthews, T., Byrne, M., Horton, R., Murphy, C., Pielke, R., Sr., Raymond, C., et al. (2022). Latent heat must be visible in climate communications. *WIREs Climate Change*, *13*(4), e779. https://doi.org/10.1002/wcc.779

McKinnon, K. A., & Poppick, A. (2020). Estimating changes in the observed relationship between humidity and temperature using noncrossing quantile smoothing splines. *Journal of Agricultural, Biological, and Environmental Statistics*, *25*(3), 292–314. https://doi.org/10.1007/s13253-020-00393-4

Miralles, D. G., Teuling, A. J., van Heerwaarden, C. C., & Vilà-Guerau de Arellano, J. (2014). Mega-heatwave temperatures due to combined soil desiccation and atmospheric heat accumulation. *Nature Geoscience*, *7*(5), 345–349. https://doi.org/10.1038/ngeo2141

Mora, C., Dousset, B., Caldwell, I. R., Powell, F. E., Geronimo, R. C., Bielecki, C. R., et al. (2017). Global risk of deadly heat. *Nature Climate Change*, *7*(7), 501–506. https://doi.org/10.1038/nclimate3322

Pal, J. S., & Eltahir, E. A. B. (2016). Future temperature in southwest Asia projected to exceed a threshold for human adaptability. *Nature Climate Change*, *6*(2), 197–200. https://doi.org/10.1038/nclimate2833

Perkins, S. E., Alexander, L. V., & Nairn, J. R. (2012). Increasing frequency, intensity and duration of observed global heatwaves and warm spells. *Geophysical Research Letters*, *39*, L20714. https://doi.org/10.1029/2012GL053361

Perron, M., & Sura, P. (2013). Climatology of non-Gaussian atmospheric statistics. *Journal of Climate*, *26*(3), 1063–1083. https://doi.org/10.1175/JCLI-D-11-00504.1

Rastogi, D., Lehner, F., & Ashfaq, M. (2020). Revisiting recent U.S. Heat waves in a warmer and more humid climate. *Geophysical Research Letters*, *47*(9), e2019GL086736. https://doi.org/10.1029/2019GL086736

Raymond, C., Matthews, T., & Horton, R. M. (2020). The emergence of heat and humidity too severe for human tolerance. *Science Advances*, *6*(19), eaaw1838. https://doi.org/10.1126/sciadv.aaw1838

Raymond, C., Matthews, T., Horton, R. M., Fischer, E. M., Fueglistaler, S., Ivanovich, C., et al. (2021). On the controlling factors for globally extreme humid heat. *Geophysical Research Letters*, *48*(23), e2021GL096082. https://doi.org/10.1029/2021GL096082

Raymond, C., Singh, D., & Horton, R. M. (2017). Spatiotemporal patterns and synoptics of extreme wet-bulb temperature in the contiguous United States. *Journal of Geophysical Research: Atmospheres*, *122*(24), 13108–13124. https://doi.org/10.1002/2017JD027140

Raymond, C., Waliser, D., Guan, B., Lee, H., Loikith, P., Massoud, E., et al. (2022). Regional and elevational patterns of extreme heat stress change in the US. *Environmental Research Letters*, *17*(6), 064046. https://doi.org/10.1088/1748-9326/ac7343

Robine, J.-M., Cheung, S. L. K., Le Roy, S., Van Oyen, H., Griffiths, C., Michel, J.-P., & Herrmann, F. R. (2008). Death toll exceeded 70,000 in Europe during the summer of 2003. *Comptes Rendus Biologies*, *331*(2), 171–178. https://doi.org/10.1016/j.crvi.2007.12.001

Ruff, T. W., & Neelin, J. D. (2012). Long-tails in regional surface temperature probability distributions with implications for extremes under global warming. *Geophysical Research Letters*, *39*, L04704. https://doi.org/10.1029/2011GL050610

Saeed, F., Schleussner, C.-F., & Ashfaq, M. (2021). Deadly heat stress to become commonplace across South Asia already at 1.5°C of global warming. *Geophysical Research Letters*, *48*(7), e2020GL091191. https://doi.org/10.1029/2020GL091191

Santer, B. D., Mears, C., Wentz, F. J., Taylor, K. E., Gleckler, P. J., Wigley, T. M. L., et al. (2007). Identification of human-induced changes in atmospheric moisture content. *Proceedings of the National Academy of Sciences*, *104*(39), 15248–15253. https://doi.org/10.1073/pnas.0702872104

Schär, C. (2016). The worst heat waves to come. *Nature Climate Change*, *6*(2), 128–129. https://doi.org/10.1038/nclimate2864

Seneviratne, S. I., Corti, T., Davin, E. L., Hirschi, M., Jaeger, E. B., Lehner, I., et al. (2010). Investigating soil moisture–climate interactions in a changing climate: A review. *Earth-Science Reviews*, *99*(3), 125–161. https://doi.org/10.1016/j.earscirev.2010.02.004

Seneviratne, S. I., Donat, M. G., Pitman, A. J., Knutti, R., & Wilby, R. L. (2016). Allowable CO_2 emissions based on regional and impact-related climate targets. *Nature*, *529*(7587), 477–483. https://doi.org/10.1038/nature16542

Sherwood, S. C., & Huber, M. (2010). An adaptability limit to climate change due to heat stress. *Proceedings of the National Academy of Sciences*, *107*(21), 9552–9555. https://doi.org/10.1073/pnas.0913352107

Simolo, C., Brunetti, M., Maugeri, M., & Nanni, T. (2011). Evolution of extreme temperatures in a warming climate. *Geophysical Research Letters*, *38*, L16701. https://doi.org/10.1029/2011GL048437

Simolo, C., Brunetti, M., Maugeri, M., Nanni, T., & Speranza, A. (2010). Understanding climate change–induced variations in daily temperature distributions over Italy. *Journal of Geophysical Research*, *115*(D22), D22110. https://doi.org/10.1029/2010JD014088

Skinner, C. B., Poulsen, C. J., & Mankin, J. S. (2018). Amplification of heat extremes by plant CO_2 physiological forcing. *Nature Communications*, *9*(1), 1094. https://doi.org/10.1038/s41467-018-03472-w

Speizer, S., Raymond, C., Ivanovich, C., & Horton, R. M. (2022). Concentrated and intensifying humid heat extremes in the IPCC AR6 regions. *Geophysical Research Letters*, *49*(5), e2021GL097261. https://doi.org/10.1029/2021GL097261

van Oldenborgh, G. J., Philip, S., Kew, S., van Weele, M., Uhe, P., Otto, F., et al. (2018). Extreme heat in India and anthropogenic climate change. *Natural Hazards and Earth System Sciences*, *18*(1), 365–381. https://doi.org/10.5194/nhess-18-365-2018

Vanos, J. K., Baldwin, J. W., Jay, O., & Ebi, K. L. (2020). Simplicity lacks robustness when projecting heat-health outcomes in a changing climate. *Nature Communications*, *11*(1), 6079. https://doi.org/10.1038/s41467-020-19994-1

Vecellio, D. J., Wolf, S. T., Cottle, R. M., & Kenney, W. L. (2022). Evaluating the 35°C wet-bulb temperature adaptability threshold for young, healthy subjects (PSU HEAT Project). *Journal of Applied Physiology*, *132*(2), 340–345. https://doi.org/10.1152/japplphysiol.00738.2021

Wang, P., Leung, L. R., Lu, J., Song, F., & Tang, J. (2019). Extreme wet-bulb temperatures in China: The significant role of moisture. *Journal of Geophysical Research: Atmospheres*, *124*(22), 11944–11960. https://doi.org/10.1029/2019JD031477

Wang, X.-S., He, L., Ma, X.-H., Bie, Q., Luo, L., Xiong, Y.-C., & Ye, J.-S. (2022). The emergence of prolonged deadly humid-heatwaves. *International Journal of Climatology*, *n/a*(n/a), 8607–8618. https://doi.org/10.1002/joc.7750

Wehner, M., Stone, D., Krishnan, H., AchutaRao, K., & Castillo, F. (2016). 16. The deadly combination of heat and humidity in India and Pakistan in summer 2015. *Bulletin of the American Meteorological Society*, *97*(12), S81–S86. https://doi.org/10.1175/BAMS-D-16-0145.1

Wheeler, P. E. (1991). The thermoregulatory advantages of hominid bipedalism in open equatorial environments: The contribution of increased convective heat loss and cutaneous evaporative cooling. *Journal of Human Evolution*, *21*(2), 107–115. https://doi.org/10.1016/0047-2484(91)90002-D

Willett, K. M., Gillett, N. P., Jones, P. D., & Thorne, P. W. (2007). Attribution of observed surface humidity changes to human influence. *Nature*, *449*(7163), 710–712. https://doi.org/10.1038/nature06207

Zelinka, M. D., Myers, T. A., McCoy, D. T., Po-Chedley, S., Caldwell, P. M., Ceppi, P., et al. (2020). Causes of higher climate sensitivity in CMIP6 models. *Geophysical Research Letters*, *47*(1), e2019GL085782. https://doi.org/10.1029/2019GL085782

Zhang, B., Linz, M., & Chen, G. (2022). Interpreting observed temperature probability distributions using a relationship between temperature and temperature advection. *Journal of Climate*, *35*(2), 705–724. https://doi.org/10.1175/JCLI-D-20-0920.1

Zhang, Y., Held, I., & Fueglistaler, S. (2021). Projections of tropical heat stress constrained by atmospheric dynamics. *Nature Geoscience*, *14*(3), 133–137. https://doi.org/10.1038/s41561-021-00695-3

Zhao, Y., Ducharne, A., Sultan, B., Braconnot, P., & Vautard, R. (2015). Estimating heat stress from climate-based indicators: Present-day biases and future spreads in the CMIP5 global climate model ensemble. *Environmental Research Letters*, *10*(8), 084013. https://doi.org/10.1088/1748-9326/10/8/084013

Zscheischler, J., & Seneviratne, S. I. (2017). Dependence of drivers affects risks associated with compound events. *Science Advances*, *3*(6), e1700263. https://doi.org/10.1126/sciadv.1700263